# Dalton Transactions

Accepted Manuscript



This is an *Accepted Manuscript*, which has been through the Royal Society of Chemistry peer review process and has been accepted for publication.

*Accepted Manuscripts* are published online shortly after acceptance, before technical editing, formatting and proof reading. Using this free service, authors can make their results available to the community, in citable form, before we publish the edited article. We will replace this *Accepted Manuscript* with the edited and formatted *Advance Article* as soon as it is available.

You can find more information about *Accepted Manuscripts* in the Information for Authors.




ROYAL SOCIETY OF CHEMISTRY

www.rsc.org/dalton

Journal Name RSCPublishing

ARTICLE

# Highly NIR emitting lanthanide complexes with 2-(tosylamino)benzylidene-N-benzoylhydrazone

Cite this: DOI: 10.1039/x0xx00000x

Received 00th January 2012,
Accepted 00th January 2012

DOI: 10.1039/x0xx00000x

www.rsc.org/

V.V. Utochnikova,[a,b] A. D. Kovalenko,[a] A.S. Burlov[c], L. Marciniak[d], I. V. Ananyev[e], A. S. Kalyakina[a], N. A. Kurchavov[f], and N. P. Kuzmina[a]

New NIR emitting materials were found among the lanthaninde complexes with 2-(tosylamino)benzylidene-N-benzoylhydrazone. Complexes of $Nd^{3+}$, $Er^{3+}$ and $Yb^{3+}$, as well as $Eu^{3+}$, $Gd^{3+}$ and $Lu^{3+}$, were synthesized for the first time. Thanks to the absence of the vibration quenching ytterbium complex was found to exhibit the photoluminescence quantum yield of 1.4%. Since sensibilization efficiency was calculated to be 55%, the losses in the quantum yield are probably due to Yb-Yb resonant energy transfer.

## Introduction

Luminescent lanthanide(III)-containing materials have recently attracted increasing attention, for example, as luminescent probes for cell imaging and medical diagnostics, due to their unique optical properties such as well-characterized and intense line-like emission, constant position of luminescence bands, long lifetimes of the excited state and high Stokes shift [1-3]. Such lanthanide materials, emitting in the near-infrared (NIR) range, are especially important for both bioanalyses and bioimaging, since NIR range has few interferences with biomaterials so that photons can penetrate deeply into biological samples, cells and tissues [1-3]. However, the efficiency of the NIR emitting lanthanide CCs luminescence is still very low [4-6].

Attempts to increase the quantum yield of NIR emitting lanthanide complexes were taken by using ligands of different classes for luminescence sensibilization, and particular success were quinoline [4, 7-9] and porfirin [5] derivatives. In complexes with porphirine lanthanides were coordinated both “within” the porphirine cavity and by an external coordination site. The highest quantum yields among the different complexes of NIR emitting lanthanides were obtained for ytterbium compounds, which has the highest gap between the lowest lying excited state and the highest sublevel of the ground state. Nevertheless even ytterbium complex quantum yields in powder state typically lay much below 1% if not lower with only few examples exceeding this value [10-11].

The above mentioned classes of compounds, as well as others with competing quantum yields [6], have two features in common: first, they have relatively low lying triplet state energy, so that ligand to metal energy transfer is rather effective. Second, and probably more important, is that chelating and bulky nature of these ligands does not allow any quenching by solvent molecules in the lanthanide coordination environment. Indeed, not only overall, but also intrinsic quantum yield of lanthanide NIR emitting complexes is rather low, i.e. it is even more important to avoid quenching than to increase the energy transfer efficiency.

Schiff bases (SBs) form another prospective class of high denticity ligands which may form solvent-free complexes [12-14]. Because of the low lanthanide affinity to nitrogen they are more often obtained as $Zn_nLn_m$ heterometallic luminescent complexes [15-17], though luminescent homometallic complexes are also well-known [18-20]. Important is that lanthanide complexes with SB ligands often include inorganic anions as chloride or nitrate. Among these ligands N-substituted (2-tosylamino)benzilideneimines are very interesting. These compounds as well as their d-metal complexes are known to possess fluorescence [21-23], though were never tested as ligands to form lanthanide complexes.

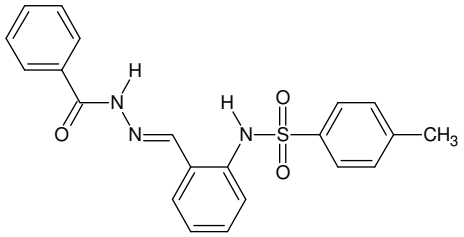


**Fig. 1 The structural formula of the HL ligand**

We have selected one of these ligands HL (Fig. 1) with N-(phenylcarbonyl) as an N-substituent, that provides additional oxygen atom able to coordinate lanthanide ion thus stabilizing the complex.

We present herein the synthesis of lanthanide complexes $Ln_2L_3X_3$ (Ln = Nd, Eu, Gd, Er, Yb, Lu; X = $NO_3$, Cl) (HL is shown in Fig. 1), their photophysical characteristics and primary investigation of luminescence in NIR range. Paramagnetic neodymium, erbium and ytterbium have been chosen as they possess metal-centered luminescence in NIR range, while europium was selected for its isotopic distribution allows using MALDI mass-spectrometry. Gadolinium complexes are suitable for estimating the excited state energy of the ligand, and diamagnetic lutetium complexes are

suitable to get the reference NMR spectra for comparison with the spectra of paramagnetic metal complexes.

## Results and Discussion

### Synthesis and characterization of potassium salt KL

With the aim to obtain lanthanide complexes with HL ligand in its deprotonated form the standard ligand exchange reaction was chosen:

$$LnX_3{\cdot}6H_2O + 3\ KL{\cdot}H_2O \rightarrow LnX_3 + 3KX \qquad (1)$$

Solid salt KL was obtained by reaction of HL with KOH in ethanol, isolated and identified based on IR, NMR and elemental analysis, and its crystal structure was determined by single crystal X-ray analysis (Fig. 3).

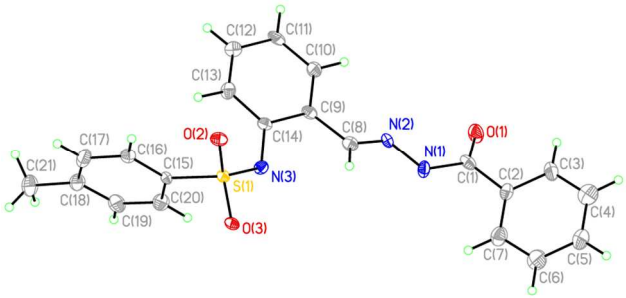


**Fig. 2. Anionic moiety in the KL crystal with the representations of non-hydrogen atoms by probability ellipsoids of atomic displacements (p = 0.5)**

The crystal structure of the KL salt is to some extent expected due to a large cation size and a number of donor atoms in the L ligand (Fig. 2) giving multiple coordination modes of the latter. There are four potassium ions (K1-K4), four ligands L being slightly different by geometry and two water molecules in the independent unit. Despite the similarity of the potassium coordination environment which is always composed by four ligands L and the water molecule, cations can be divided into two groups by coordination polyhedron type (Fig. 4). Thus, cations K1 and K4 have strongly distorted trigonal-prismatic environment which is composed by four oxygen atoms of the ligands, the water molecule and the N2 nitrogen atom of the ligands (Fig. 4a and 4c). At the same time the K2 and K3 cations are both coordinated by N2 and N3 nitrogen atoms that together with five oxygen atoms of the ligands and the water molecule give distorted tetragonal-prismatic environment in this case (Fig. 4b and 4d).

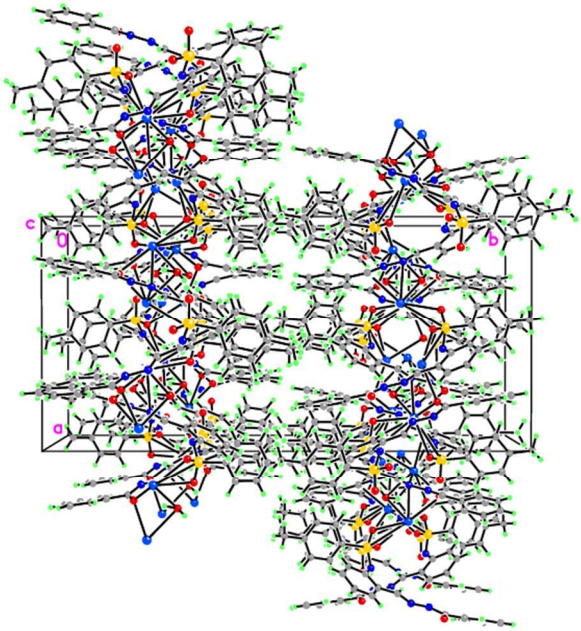


**Fig. 3. Layered structure of KL in the crystal**

According to an analysis of metal-ligand distances (Table 1) and a Cambridge Structural Database (CSD) [24] search for K-O and K-N bonding distances the metal-ligand bonding for cations with the same polyhedron is similar. Cations with less coordination number (K1 and K4) form rather strong K-O bond with the sulfonyl group of the ligand (2.625(4) and 2.633(4) Å for K1 and K4 respectively), three K-O bonds of intermediate strength with the carbonyl oxygen atom and the water molecule (2.784(5)-2.834(5) Å for K1 and 2.774(4)-2.883(5) Å for K4) and weaker K-O interaction with the sulfonyl group (2.962(4) and 3.085(4) Å for K1 and K4 correspondingly). The coordination number of six is achieved by the presence of an extremely weak K-N2 interaction (3.317(5) and 3.325(5) Å for K1 and K4 respectively).

**Table 1. The geometric peculiarities of metal-ligand bonding in the KL crystal.**

| | K1 | K4 | K2 | K3 |
|---|---|---|---|---|
| O1 | 2.784(5), 2.834(5) | 2.814(5), 2.883(5) | 2.783(4), 2.964(5) | 2.732(4), 2.876(5) |
| O2 | 2.625(4) | - | 3.030(4) | 2.712(4) |
| O3 | 2.962(4) | 2.633(4), 3.085(4) | 2.713(4), 2.747(4) | 2.763(4), 3.155(4) |
| O1w | - | 2.774(4) | - | 2.763(4) |
| O2w | 2.787(5) | - | 2.737(4) | - |
| N2 | 3.317(5) | 3.325(5) | - | 3.288(5) |
| N3 | - | - | 2.945(5), 3.340(5) | 2.925(5) |
| Polyhedron | Distorted trigonal prism | | Distorted tetragonal prism | |

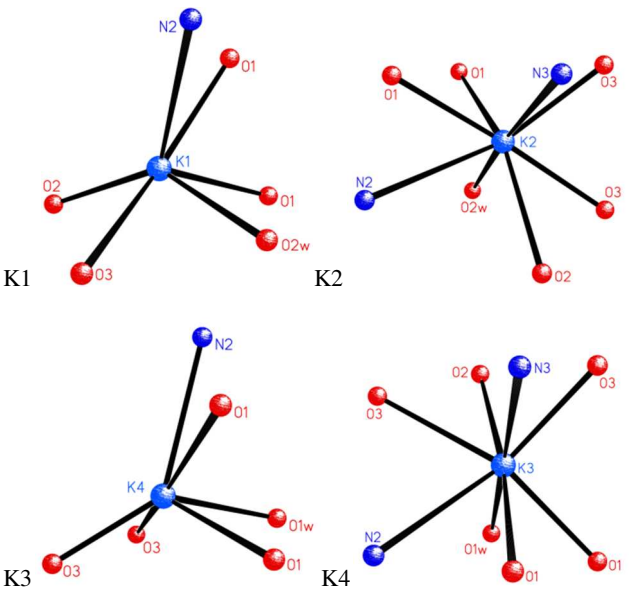


**Fig. 4. Coordination environment of the K1 (a), K2 (b), K4 (c), K3 (d) potassium ions in the crystal of KL. Letter 'w' denotes oxygen atoms of water molecules**

On contrary there is no short K-O bonds in the case of K2 and K3 cations that is compensated by more number of weak (2.964(5)-3.155(4) Å) and intermediate K-O bonds and the presence of rather short K-N3 interactions (2.945(5) and 2.925(5) Å for K2 and K3 respectively). Again, the weakest cation-anion interactions are observed for sulfonyl group (K3-O3 3.155(4) Å) and nitrogen atoms (K2-N3 3.340(5) Å and K3-N2 3.288(5) Å). Note that according to geometric criteria the N1 amide nitrogen atom does not participate in metal-ligand bonding in all cases that is in line with the CSD search of a fragment containing both the potassium atom and the amide group: thus, the amide nitrogen atom is coordinated to metal in only 13 structures from 680 hits.

In crystal any ligand L possesses bridging function giving endless chains of tetramer units in which two types of cation polyhedrons alternates (Fig. 4). Such chains are additionally stabilized by water molecules being bridging ligands between K1 and K2 or K4 and K3 cations, which is in line with less metal…metal separations in these fragments: K1…K2 3.60 Å, K2…K4 4.52 Å, K4…K3 3.64 Å, K3…K1 4.42 Å. Polymeric chains of KL are in turn bounded by bridging L ligands into layers (Fig. 3), so that K1 and K2 atoms from one chain are cross-linked with K3 and K4 of the neighbor chain by the ligand bridging groups, and K2 and K3 atoms of one chain are cross-linked to K4 and K1 atoms of the neighbor chain. Bulky ligands result in large distance between the chains being 9.0 Å. A number of weak H…H and C-H…π interactions between layers stabilize three-dimensional crystal structure.

Powder XRD patterns of KL were compared with the calculated powder diffraction data from single crystal (Fig. S1). It is obvious that the patterns coincide, indicating the same crystal structure of KL in polycrystalline powder and in single crystals. No additional reflexes, corresponding to HL impurity, were revealed.

**NMR spectroscopy** To determine which proton of HL removes under deprotonation and formation of KL, the data of $^1$H NMR spectra, together with 2D NMR COSY and NOESY spectra, were obtained and compared with HL spectra. As expected, in $^1$H NMR spectra of HL and KL the resonance signals, corresponding to the hydrogen atom in NH groups (11.1 and 12.1 ppm for HL; 11.7 ppm for KL) and to the methylene group (8.5 ppm for HL; 9.1 ppm for KL) are observed. The disappearance of one of the NH resonance signals and shift of the other one together with upfield shift of methylene signal in potassium salt spectrum is indicative of the deprotonation of HL (Fig. 5).Signals in the aromatic area (6-8 ppm) were initially assigned based on analysis of the integral intensity and signal splitting that depends on the proton environment (Fig. 5, right).

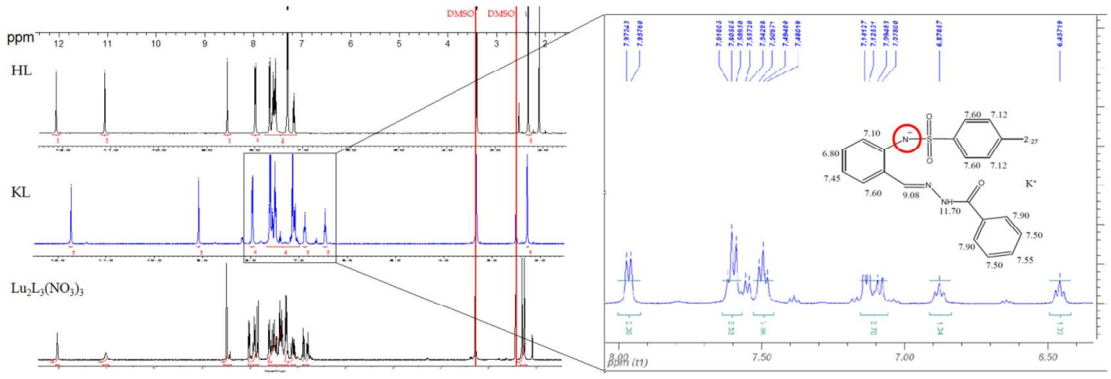


**Fig. 5. a) $^1$H NMR spectra of HL, KL and $LuL_3(NO_3)_3$ and b) $^1$H**

Based on these data further assignment was run according to COSY and NOESY spectra, that show through-bond and through-space contacts (Fig. S2, Fig. S3). It also allows to assign the signal at 11.7 ppm to the =N-NH-C(O)- group, witnessing the deprotonation of the tosyl-bonded NH group.

So, the interaction of HL with KOH results in deprotonation of the tosyl-bonded NH group and formation of potassium salt KL with polymeric structure.

**Synthesis and characterization of lanthanide salts $Ln_2L_3X_3$ (Ln = Nd, Eu, Gd, Er, Yb, Lu; X = $NO_3$, Cl)**

The interaction of stoichiometric amounts of KL and hydrates of lanthanide chloride or nitrate (reaction 1) resulted surprisingly in formation of $Ln_2L_3X_3$ complexes, ascribed according to the scheme:

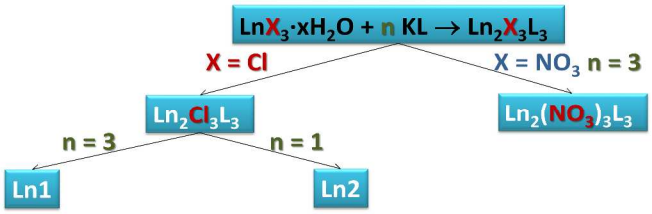


Independently on the reagent ratio (n=3 or n=1) the product composition corresponded to the $Ln_2L_3X_3$ for both X= Cl and $NO_3$. Nevertheless XRD patterns of **Ln1** and **Ln2** were remarkably different, though there were no traces neither of initial KL nor of HL, as it is shown on example of **Er1** and **Er2** on Fig. 6.

XRD patterns of the complexes within each of **Ln1** and **Ln2** series coincide (Fig. S4).

In spite of the same *brutto* composition, crystal structures of **Ln1** and **Ln2** are obviously different, so it is essential to check if **Ln1** and **Ln2** form individual phases and if their photophysical properties are affected by this phase difference. As far as all the obtained products were found to have very low solubility in organic solvents (ethanol, acetone, $CHCl_3$, *i*-PrOH, acetonitrile and their mixtures), no single crystals were obtained, and thus in the absence of the structural data the individuality of $Ln_2L_3X_3$ complexes has been proven by combination of indirect methods, i.e. elemental analysis, XRD, IR spectroscopy, TGA, MALDI, NMR spectroscopy and luminescent spectroscopy.

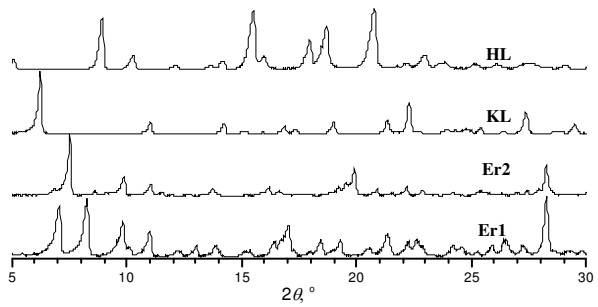


**Fig. 6. XRD patterns of HL, KL, Er1 and Er2**

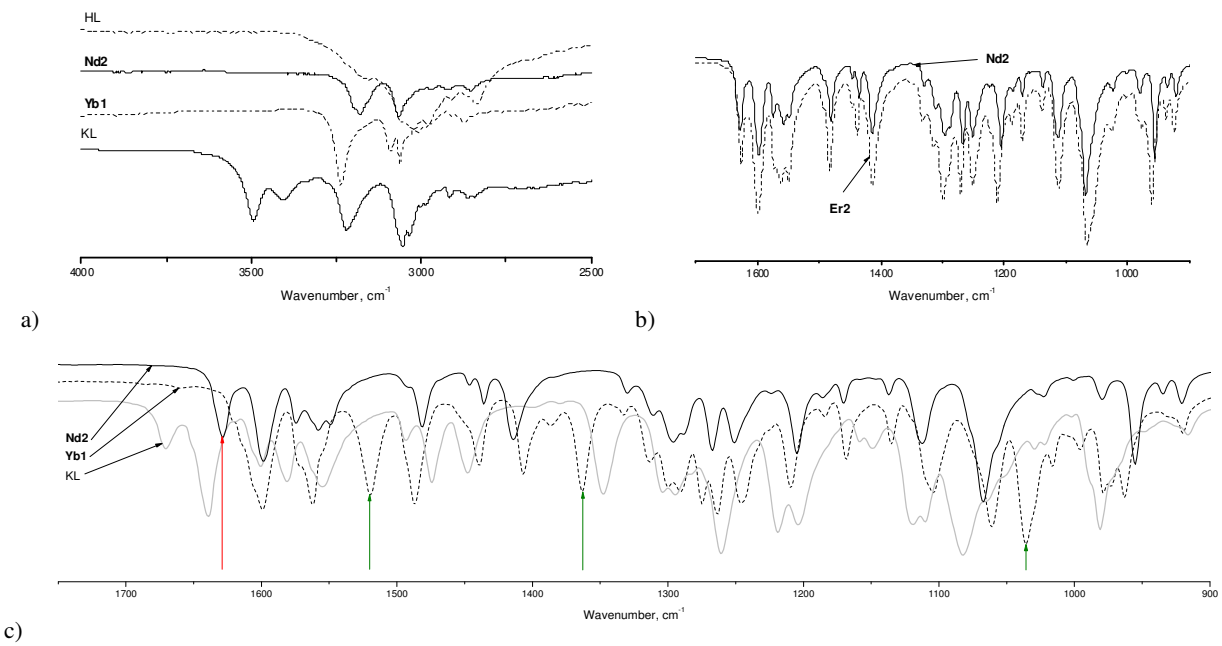


**Fig. 7. IR spectra of a) HL, KL, Yb1, b) Er1 and Nd2, and c) KL, Nd2 and Yb1**

**Table 2.** The most important characteristic bands of HL, KL and $LuL_3(NO_3)_3$

| Cmpnd | Vibration frequency, $cm^{-1}$ | | | | | | | |
|---|---|---|---|---|---|---|---|---|
| | ν(NH) | ν(CH) | Amide I | Amide II | Amide III | ν(C=C) | ν($NO_3$) | ν($SO_2$) |
| HL | 3159-2837 | | 1645 | 1548 | 1290 | 1608 | - | 1154 |
| KL | 3218 | 3060-2853 | 1639 | 1553 | 1296 | 1602 | - | 1118 |
| $LuL_3(NO_3)_3$ | 3210 | 3070-2853 | 1615* | 1564 | 1300 | 1601 | 1440 | 1108 |

| | | | | | | | | |
|---|---|---|---|---|---|---|---|---|
| **Yb1** | 3239 | 2831-3128 | 1621* | 1562 | 1300 | 1599 | - | 1101 |
| **Nd2** | 3182 | 2812-3112 | 1629 | 1557 | 1297 | 1598 | - | 1112 |
| **Er2** | 3181 | 2812-3117 | 1627 | 1563 | 1300 | 1600 | - | 1112 |

* present as a shoulder to the ν(C=C)

**IR spectroscopy** IR spectra of $Ln_2L_3(NO_3)_3$, **Ln1** and **Ln2** were compared with those of HL and of KL (Fig. S6). The complicity of the ligand together with the variation of the coordination modes observed for KL makes IR spectra very complex and hard for interpretation, therefore only the most informative bands were selected for further analysis (Table 2). No ν(OH) band was found in the spectra of these complexes, indicating the absence of the coordinated solvent. It is also witnessed by the absence of the weight loss on the TG curves of the complexes (Fig. S5).

Further comparison of IR spectra within **Ln1** and **Ln2** series indicate no difference, which is shown in Fig. 7b on example of **Er2** and **Nd2**. Nevertheless in the IR spectra of the samples of different series **Ln1** and **Ln2** the minimal differences appear (3-4 bands) which origin demands additional study (Fig. 7c). Important is however that among those differences is the first amide band (1627-1629 $cm^{-1}$) which is present in the spectra of **Ln2**, but is only shown as a part of broad band (amide 1 + ν(C=C)) in the spectra of **Ln1** and $LuL_3(NO_3)_3$. The same differences are also observed on the Raman spectra (Fig. S7).

**MALDI spectroscopy** Because of the specific isotopic distribution europium complexes were used for MALDI spectroscopy. MALDI spectrum of **Eu2** revealed the presence of both monomeric ($[EuL]^+$, $[EuL_2]^+$, $[EuL_2\text{-}H+Na]^+$, $[EuL_2\text{-}H+K]^+$, $[EuL_2\text{-}2H+2K]^+$) and dimeric molecular ions ($[Eu_2L_3]^+$, $[Eu_2L_3+H+K]^+$) (Fig. 8a), suggesting that **Eu2** has at least dimeric structure. However the presence of several sodium and particular potassium containing species signals, including an intense one at 973/975 m/z, demanded assignment verification. Therefore $Eu_2L_3(NO_3)_3$ was used instead of $Eu_2L_3Cl_3$ (**Eu2**), since atomic mass of chlorine isotopes (35 and 37 amu) is close to the one of potassium (39 amu).

The spectrum of $Eu_2L_3(NO_3)_3$ revealed essentially the same signals of monomeric units (Fig. 8b), the most intensive of $[EuL_2]^+$, $[EuL_2\text{-}H+Na]^+$, $[EuL_2\text{-}H+K]^+$, $[EuL_2\text{-}2H+2K]^+$ species, proving the correct assignment. Besides several nitrate containing species signals were detected, including monomeric ($[EuL_2(NO_3)]^+$) and dimeric ($[Eu_2L_2(NO_3)]^+$). Besides nitrate-free dimeric $[Eu_2L_2]^+$ and even trimeric $[Eu_3L_2]^+$ ion signal was detected, confirming at least oligomeric structure of the complex, and more probably even polymeric, taking into account its very low solubility, as was found in [25].

**NMR spectroscopy** NMR spectroscopic study of paramagnetic ion complexes was run in comparison with analogous lutetium complexes **Lu2** and $Lu_2L_3(NO_3)_3$ complexes.

Comparison of $^1H$ NMR spectra of $Lu_2L_3(NO_3)_3$ and KL (Fig. 5) revealed a downfield shift of the methylene signal together with the rearrangement of the proton signals in the aromatic part of the spectrum, that arises from different ligand coordination modes. Besides signals of both NH groups with summary integral intensity 1 are observed instead of one signal, indicating two resonance forms of the ligand in the complex. The same features are observed in the spectrum of **Lu2**, both spectra almost coincide (Fig. 9).

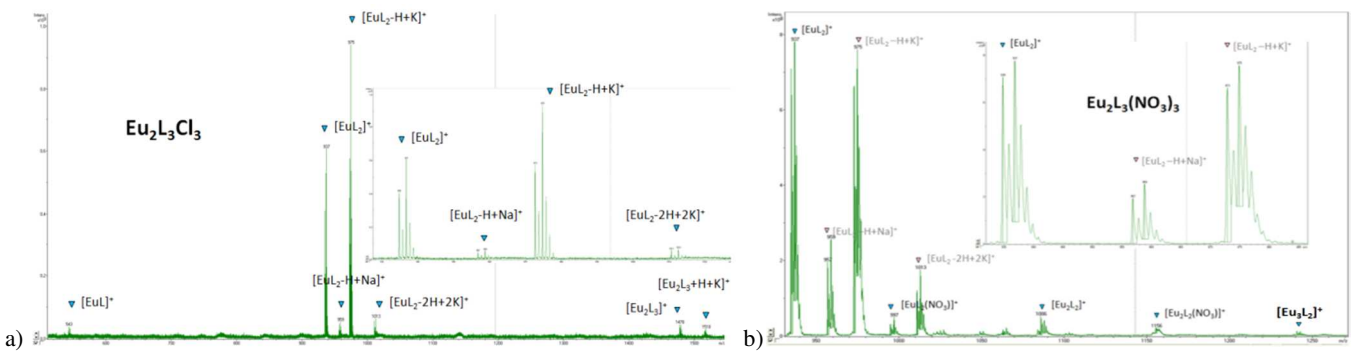


**Fig. 8. MALDI mass-spectra of a) Eu2 and b) $Eu_2L_3(NO_3)_3$**

Journal Name RSCPublishing

ARTICLE

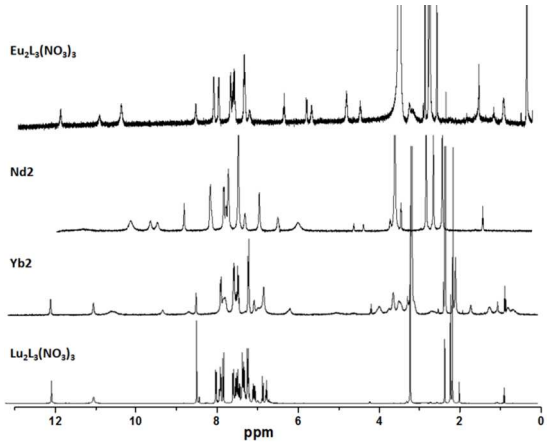


**Fig. 9. $^1$H NMR spectra of Lu2, Yb2, $Lu_2L_3(NO_3)_3$ and $Eu_2L_3(NO_3)_3$. Intensive signals at 2.5 and 3.2 ppm are from DMSO.**

The NMR spectra of $Eu_2L_3(NO_3)_3$, **Yb1** and **Nd2** are more complex, demonstrating both signal pseudocontact shifts (PCS) and widening due to paramagnetic relaxation enhancement (PRE) (Fig. 9), which is the highest for **Nd2** and the lowest for $Eu_2L_3(NO_3)_3$ due to the highest and the lowest PRE radii [26]. Both upfield and downfield shifts of aromatic signals are observed for both $Eu_2L_3(NO_3)_3$ **Yb1** and **Nd2** (Fig. 9), which is due to different spatial location of the corresponding protons with respect to the paramagnetic metal ion. The appearance of the shift and widening is an indirect proof of non-dissociated complex presence in DMSO-d$^6$ solution.

So, the reaction of lanthanide chloride or nitrate with KL resulted in the formation of $Ln_2L_3X_3$ (X = $NO_3$, Cl) independently on the reagent ratio. Some differences nevertheless seem to occur between **Ln1** and **Ln2**, which is indicated by the differences of the XRD patterns and in the IR spectra.

**Luminescence spectroscopy** Luminescent properties were first examined for HL, KL, $Lu_2L_3(NO_3)_3$ and **Gd2**, which luminescence originates from the organic part of the molecule, and then for **Yb1**, **Yb2**, **Er2** and **Nd2**, where ionic luminescence in the NIR range was studied. Both **Yb1** and **Yb2** were taken to compare if the photophysical properties are affected by the change in the crystal structure.

As expected, KL exhibits a broad luminescence band corresponding to the emission of organic part of the molecule (Fig. 10). Hypsochromic shift of the spectrum and FWHM decrease upon deprotonation is due to molecule rigidity. Absence of HL luminescence band on the KL luminescence spectrum is another witness of product purity.

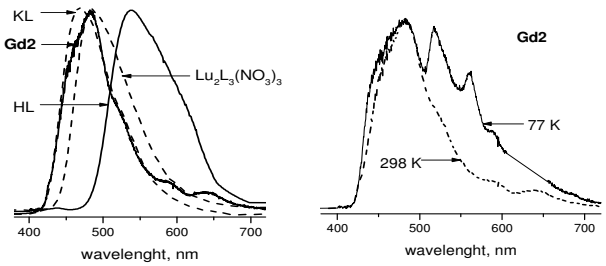


**Fig. 10. Luminescence spectra of HL, KL, Gd2 and $LuL_3(NO_3)_3$ at 298 K (left) and Gd2 at 298 K and 77K (right)**

Luminescence spectra of both **Gd2** and **Lu2** at room temperature also consisted of one fluorescence band with the maxima at 485 nm. Luminescence spectrum of **Lu2** remains the same at 77K, though phosphorescence bands appear in the one of **Gd2** (Fig. 10, right), allowing to estimate ligand excited states as $S_1(L^-)$ = 20600 cm$^{-1}$ and $T_1(L^-)$=19400 cm$^{-1}$. The excited state lifetime of **Gd2**, measured upon triplet state relaxation, is equal to 41,3(5) μsec. It is worth noting that the $\Delta E(S_1\text{-}T_1)$ = 1200 cm$^{-1}$ is very low, which allows to suggest **Gd2** as potential material with delayed fluorescence [27]. Such a behaviour in turn may be explained by different spatial localization of HOMO and LUMO.

The luminescence spectra of **Nd2**, **Er2** and **Yb2** revealed typical ionic luminescence, which resolution significantly increases at 77K (Fig. 11, Fig. 12). The highest intensity was observed for ytterbium complexes, therefore they were examine in more details. So, luminescence spectra at 298K and 77K, excited state lifetimes and quantum yields were compared for **Yb2** and **Yb1**.

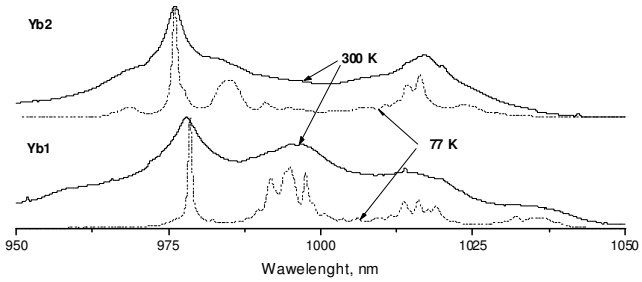


**Fig. 11 Luminescence spectra of Yb1 and Yb2 at room temperature and at 77 K**

Journal Name RSCPublishing

ARTICLE

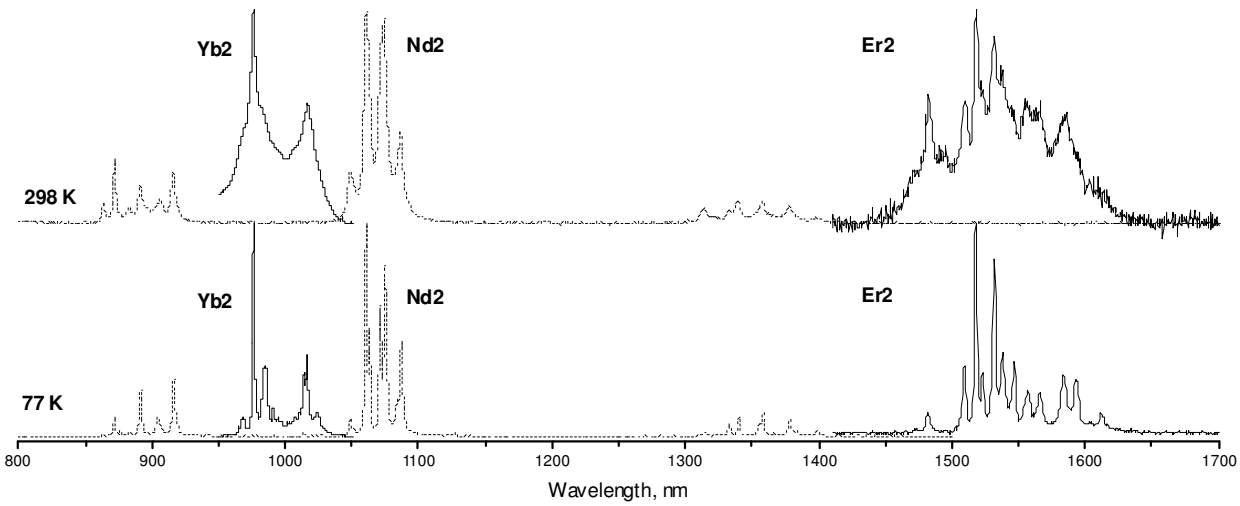


**Fig. 12 Luminescence spectra of Nd2, Er2 and Yb2 at room temperature and at 77 K**

The luminescence spectra of both **Yb1** and **Yb2** revealed typical ionic luminescence, corresponding to the $^2F_{7/2}\rightarrow{}^2F_{5/2}$ transition (Fig. 11) upon through-ligand excitation. As expected, different Stark splitting of the luminescence band was observed for **Yb1** and **Yb2**, indicating different coordination environment, which is consistent with the differences in IR spectra.

Nevertheless the lifetimes of the excited $^2F_{7/2}$ state of $Yb^{3+}$ as well as were found to be practically the same for both complexes at 298 K as well as at 77 K, indicating that excited state relaxation processes are the same for both compounds. Luminescence quantum yields measured for **Yb1** and **Yb2** also coincided and reached 1.2% and 1.4%, correspondingly.

**Table 3. Photophysical data of Yb1 and Yb2**

| Compound | $\tau_{obs}$, μsec | | PLQY, % |
|---|---|---|---|
| | 298 K | 77 K | |
| **Yb1** | 47.8 | 49.7 | 1.2 |
| **Yb2** | 48.0 | 48.7 | 1.4 |

These values are rather high for ytterbium coordination compounds, which quantum yield in powder state are typically much below 1%. Nevertheless it is rather far from 100%, therefore the question arises where the losses originate from. Taking into account a big difference in the energies of ligand excited state and ytterbium resonance level (ca. 9400 $cm^{-1}$), the low quantum yield may originate from the low sensibilization efficiency, which can be estimated as

$$\eta_{sens} = Q_L^{Yb} / Q_{Yb}^{Yb},$$

where $Q_{Yb}^{Yb} = \frac{\tau_{obs}}{\tau_{rad}}$. The pure radiative lifetime $\tau_{rad}$ of $Yb^{3+}$ is believed to depend only insufficiently on coordination environment and is typically estimated as 2 ms [28], so the internal quantum yield is $Q_{Yb}^{Yb}$ =2.4%, giving rather high sensibilization efficiency $\eta_{sens}$ = 55%. The radiative lifetime can also be calculated from the absorption spectrum corresponding to the emission spectrum with the help of the modified Einstein's equation [29]:

$$\frac{1}{\tau_{rad}} = 2303 \times \frac{8\pi c n^2 \tilde{\nu}_m^{\,2}(2J+1)}{N_A(2J'+1)} \int \varepsilon(\tilde{\nu}) d\tilde{\nu}$$

where $c$ is the speed of light in vacuum (cm $sec^{-1}$), $n$ is refractive index, $N_A$ is Avogadro's number, $J$ and $J'$ are the quantum numbers for the ground and excited states, respectively, $\int \varepsilon(\tilde{\nu}) d\tilde{\nu}$ is the integrated spectrum of the f-f transition, $\tilde{\nu}_m = \frac{\int \tilde{\nu}\varepsilon(\tilde{\nu}) d\tilde{\nu}}{\int \varepsilon(\tilde{\nu}) d\tilde{\nu}}$ is the barycenter of the transition. The very low solubility of **Yb1** and **Yb2**, which was measured to be 1.6mM in MeCN, lead to the very low signal to noise ratio in the absorption spectrum (Fig. S9), so the value of $\tau_{rad}$ = 0.96 ms obtained from this spectrum is only a rough estimation. This value resulted in $Q_{Yb}^{Yb}$ =5% and $\eta_{sens}$ = 25%.

Even this value of $\eta_{sens}$ is rather high for such a big difference in the energies of ligand excited state and ytterbium resonance level, which indicates that in case of NIR emitters it is indeed much more important to exclude the possible quenchers prior to look for the ligands with low lying triplet state.

The question of the quenching origin nevertheless remains. Typically the energy losses in NIR emitting complexes are associated with the vibrational quenching, which, however, is questionable for the compounds under investigation. Indeed, the $\tau_{obs}$ is almost independent on the temperature (Fig. S8, Table 3), while the vibrational quenching is usually temperature-dependent [30-32], making the observed lifetimes also to depend on temperature.

So the remaining possibility of the quenching might be resonant Yb-Yb energy transfer. This energy transfer is well-known to quench the ytterbium luminescence in inorganic compounds, such as $Yb^{3+}$-doped garnets, YSZ etc., if the doping concentrations is higher than a certain critical value. Knowing the crystal lattice parameters one can recalculate these values into the critical distances d(Yb...Yb), which appear to be as high as 10Å [33] and even 20Å [34].

As far as **Yb1** and **Yb2** have oligo- or polymeric structure, d(Yb...Yb) in these complexes should be rather low; so, the highest K...K distance, *i.e.* the interchain distance in KL (Fig. 3), is still below 9Å, even though the bridging ligand coordinates two neighbouring potassium atoms by two different functional groups. Though we have no structural data for neither **Ln1** nor **Ln2**, we suggest that d(Yb...Yb) should not exceed this value, which depends only on the ligand geometry. So the value of d(Yb...Yb) should be below the typical critical value, making resonant Yb-Yb energy transfer the possible quenching mechanism.

## Conclusions

A series of lanthanide complexes $Ln_2L_3X_3$ with 2-(tosylamino)benzylidene-N-benzoylhydrazone were synthesized by reaction of lanthanide nitrate or chloride $LnX_3{\cdot}6H_2O$ with KL. This potassium salt KL has layered structure, each layer is buit from the polymeric chains, linked by the bridging ligands.

The composition of lanthanide complexes was shown to be independent on reagent ratio, which, however, influences their crystal structure. Data of MALDI spectroscopy and low solubility of the obtained complexes allows to suggest their oligo- or polymeric structure. Thanks to high ligand denticity all the complexes do not contained coordinated solvent molecules, which was shown to exclude vibration quenching of NIR luminescence. Quantum yield of $Yb_2L_3Cl_3$ reached 1.4%, that is remarkable for lanthanide complex based NIR emitters. Since sensibilization efficiency was calculated to be 55%, and the losses in the quantum yield are probably due to Yb-Yb resonant energy transfer. Therefore complex dilution with non-luminescent ion as in [35] or monomeric complex formation may seem a perspective approach to the synthesis of efficient NIR emitters.

## Experimental section

### Materials and methods

**Elemental analyses (C, H, N)** were performed on a Vario Micro Cube (Elementar, Germany) by the Microanalytical Service of the Lomonosov Moscow State University.
**IR spectra** were recorded on bulk samples in the range of 4000–600 $cm^{-1}$ with a Perkin-Elmer Spectrum One spectrometer equipped with a universal attenuated total reflection sampler.
**$^1$H NMR** analysis was carried out on the Avance-400 Bruker (400 MHz, DMSO-$d^6$/TMS).
**Raman spectra** were recorded in the range of 400–2000 $cm^{-1}$ with a Renishaw InVia spectrometer.
**Photoluminescence spectra** at 25 °C and 77 K in visible range were measured on multichannel spectrometer S2000 (Ocean Optics) with a diode laser ($\lambda_{ex}$ = 337 nm) as an excitation source. **Luminescence lifetimes** in visible range were determined using boxcar averager system (model 162) including gated integrators (model 164) and wide-band preamplifier (model 115) from EG&G Princeton applied research. **Lifetimes** were calculated from the luminescence kinetics recorded upon excitation with nitrogen laser (337 nm). Lifetimes are averages of at least three independent measurements. All luminescence decays proved to be perfect single-exponential functions.
**Photoluminescence spectra and lifetimes** in NIR range were measured using an Edinburgh Instruments FLS980 Fluorescence Spectrometer equipped with 450 W Xenon lamp. Both the excitation and emission 300 mm focal length monochromators were in Czerny Turner configuration. Excitation arm was supplied with holographic grating of 1800 lines/mm, blazed at 250nm. While the emission spectra was supplied with ruled grating, 1800 lines/mm blazed at 500nm. The spectral resolution was 0.1 nm. The R5509-72 photomultiplier tube from Hamamatsu in nitrogen-flow cooled housing was used as a detector for near infrared range.
**Absorption and diffuse reflection spectra** were measured in acetonitrile using Lambda950 spectrometer (Perkin Elmer).
**Quantum yields** were determined with the Fluorolog FL3–22 spectrofluoremeter at room temperature under excitation into ligand states according to an absolute method using an integration sphere. Each sample was measured three times to get an average value. The estimated error for the quantum yields is ±10%.
**X-ray powder diffraction** (XRD) measurements were performed on a Rigaku D/MAX 2500 diffractometer in the *2θ* range 5-80° with Cu Kα radiation (*λ=1,54046 Å*).
**MALDI** spectroscopy was made on Autoflex II with time of flight detector (Bruker Daltonics, Germany).
**Crystallographic data:** Crystals of the KL salt ($C_{84}H_{72}K_4N_{12}O_{14}S_4$, M = 1758.17) are monoclinic, space group $P2_1/c$, at 120K: a = 14.873(4), b = 31.050(8), c = 17.737(4), β = 90.749(5), V = 8190(3) $Å^3$, Z = 4 (Z' = 2), $d_{calc}$ = 1.426 $gcm^{-3}$, μ(MoKα) = 0.90 $cm^{-1}$, F(000) = 3648. Intensities of 55854 reflections were measured with a Bruker APEX 2 Duo diffractometer [λ(MoKα) = 0.71072Å, ω-scans, 2θ<54°] and 17806 independent reflections [$R_{int}$ = 0.1369] were used in further refinement. The structure was solved by direct method and refined by the full-matrix least-squares technique against $F^2$ in the isotropic-anisotropic approximation. The positions of all hydrogen atoms were calculated using geometric criteria and possible H-bonding network: hydrogen atoms of water molecules were not localized from different Fourier map. All hydrogen atoms were refined in the isotropic approximation within the riding model. For KL, the refinement converged to wR2 = 0.2236 and GOF = 0.988 for all independent reflections (R1 = 0.0765 was calculated against F for 9401 observed reflections with I>2σ(I)). All calculations were performed using SHELX 2014 [36].
CCDC 1054462 contains the supplementary crystallographic data for KL. These data can be obtained free of charge via http://www.ccdc.cam.ac.uk/conts/retrieving.html (or from the CCDC, 12 Union Road, Cambridge, CB21EZ, UK; or deposit@ccdc.cam.ac.uk).

**Syntheses**

**Synthesis of HL.** The synthesis of HL was performed follow the scheme:

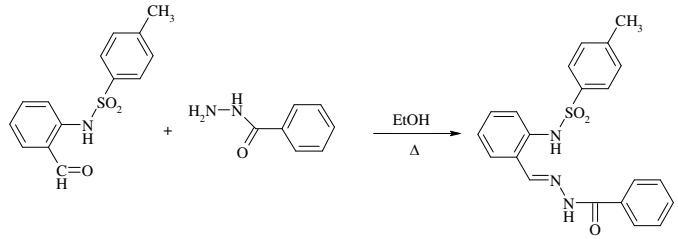


To a hot solution of 2-tosylaminobenzaldehyde (2.75 g, 10 mmol) in ethanol (50 ml) a hot solution of N-benzoylhydrazine (1.36 g, 10 mmol) in ethanol (20 ml) was added. The mixture was refluxed for 3 hours. A precipitate was filtered off and recrystallized from ethanol.

Yield 86 %. Colorless crystals, m.p. 194-195 °C.

Elemental analysis, %: clcd. C 64.11, H 4.87, N 10.68, found C 64.23, H 4.98, N 10.73

**Synthesis of KL.** Ethanol solution of KOH (1.05 mmol) was added to ethanol solution of HL (1 mmol), and the mixture was stirred for 3 hours at room temperature. The solvent was then partially evaporated to give the white precipitate of KL crystals, that were filtered off and washed thrice with a small amount of cold ethanol.

Elemental analysis, %: clcd. C 58.47 H 4.21 N 9.74 S 7.43, found C 59.11, H 4,28, N 9.55, S 7.38.

$^1$H NMR (δ, ppm, DMSO/TMS): 11.7 (s, 1H), 9.1 (c, 1H), 7.9 (c, 2H), 7,5 (d, 6H), 7.2 (d, 3H), 6.7 (s, 1H), 6.2 (s, 1H), 2.3 (s, 1H).

**Synthesis of $Ln_2L_3X_3$ (Ln = Nd, Eu, Gd, Er, Yb, Lu; X = $NO_3$, Cl)**. The reaction between ethanol solutions of lanthanide nitrate or chloride and KL resulted in the formation of white precipitate. It was filtered off, washed several times with cold ethanol and dried in dessicator.

If x=3, products were assigned **Ln1**; if x=3, products were assigned **Ln2**.

**$Er_2L_3Cl_3$**

Elemental analysis, %: clcd. C 46.72, H 3.34, N 7.79, S 5.93.

**Er1**: C 46.29, H 3.50, N 7.49, S 5.75,

**Er2**: C 46,33, H 3,43, N 7.42, S 5.12.

**$Yb_2L_3Cl_3$**

Elemental analysis, %: clcd C 46.43, H 3.31, N 7.73, S 5.90.

**Yb1**: C 45.93, H 3.14, N 7.53, S 5.32.

$^1$H NMR (δ, ppm, DMSO/TMS): 12.1, 11.1, 10.6, 9.4, 8.5, 8.0, 7.9, 7.6, 7.3, 7.1, 7.0, 6.9, 6.3, 4.3, 4.1, 3.9, 3.8, 3.6, 3.6, 3.4, 2.8, 2.2, 1.8, 1.4, 1.2, 1.0.

**Yb2**: C 45.64, H 3.31, N 7.73, S 5.90.

**$Nd_2L_3Cl_3$ = Nd1**

Elemental analysis, %: clcd C 48.12, H 3.46, N 8.02, S 6.12, found C 47.63, H 3.50, N 7.69, S 6.10.

$^1$H NMR (δ, ppm, DMSO/TMS): 10.0, 9.6, 9.4, 8.7, 8.0, 7.7, 7.6, 7.3, 7.1, 6.8, 6.3, 5.8, 4.4, 4.1, 3.5, 2.1, 1.1.

**$Gd_2L_3(NO_3)_3$**

Elemental analysis, %: clcd. C 45.09, H 3.24, N 10.02, S 5.73, found C 45.88, H 3.26, N 10.09, S 5.88.

**$Eu_2L_3(NO_3)_3$**

Elemental analysis, %: clcd. C 45.38, H 3.24, N 10.08, S 5.77, found C 45.67, H 3.19, N 10.64, S 5.32.

$^1$H NMR (δ, ppm, DMSO/TMS): 12.0, 11.0. 10.5, 8.5, 8.1, 7.9, 7.9, 7.6, 7.5, 7.3, 7.1, 6,3, 6.2, 5.7, 5.5, 4.6, 4.3, 3.0, 2.6, 2.5, 2.3, 2.0.

**$Eu_2L_3Cl_3$ = Eu2**

Elemental analysis, %: clcd. C 47.66, H 3.43, N 7.94, S 6.06, found C 47.96, H 3.69, N 7.75, S 6.10.

**$Lu_2L_3(NO_3)_3$**

Elemental analysis, %: clcd. C 44.17, H 3.18, N 9.81, S 5.61, found C 44.78, H 2.70, N 9.57, S 5.04.

$^1$H NMR (δ, ppm, DMSO/TMS): 12.1(s), 11.1(s), 8.1(s), 8.0(m), 7.8(m), 7.7(m), 7.7(m), 7.4(m), 7.3(m), 7.1(m), 6.9(m), 6.8(m), 2.3(d), 2.1(s).

**$Lu_2L_3Cl_3$**

$^1$H NMR (δ, ppm, DMSO/TMS): 12.1(s), 11.1(s), 8.5(m), 8.0(m), 7.6(m), 7.3(m), 7.1(m), 6.9(m), 6.8(m), 6.7(m), 2.3(d), 2.1(s).

## Acknowledgements

This research was supported by Russian Foundation for Basic Research (Grant Nos. 13-03-12453 and 14-03-32052).

## Notes and references

[a] M. V. Lomonosov Moscow State University, Moscow, Russian Federation.
[b] P. N. Lebedev Physical Institute, Russian Academy of Sciences, Moscow, Russian Federation
[c] Institute of Physical and Organic Chemistry, Southern Federal University, Rostov-on-Don, Russia
[d] Institute of Low Temperature and Structure Research, Polish Academy of Sciences, Wroclaw, Poland
[e] A. N. Nesmeyanov Institute of Organoelement Compounds, Russian Academy of Sciences, Moscow, Russia Federation
[f] Photochemistry Center, Russian Academy of Sciences, Moscow, Russian Federation

1. I. Hemmilä and V. Laitala, *J. Fluoresc.*, 2005, **15(4)**, 529
2. Bo Song, V. Sivagnanam, C. D. B. Vandevyver, I. Hemmilä, H.-A. Lehr, M. A. M. Gijsb and J.-C. G. Bünzli, *Analyst*, 2009, **134(10)**, 1991
3. M.Y. Berezin and S. Achilefu, *Chem. Rev.*, 2010, **110(5)**, 2641
4. F. Artizzu, M. L. Mercuri, A. Serpe, P. Deplano, *Coord. Chem. Rev.*, 2011, **255**, 2514
5. V. Bulach, F. Sguerra, M. W. Hosseini, *Coord. Chem. Rev.*, 2012, **256**, 1468
6. J.-C. G. Bünzli and S. V. Eliseeva, *J. Rare Earths*, 2010, **28(6)**, 824
7. Zh.-P. Zheng, X.-X. Zhang, T. Li, J. Yang, L.-M. Wei, L.-G. Zhang, X.-M. Lin and Y.-P. Cai, *Dalton Trans.*, 2014, **43**, 14009
8. A. Nonat, D. Imbert, J. Pecaut, M. Giraud and M. Mazzanti, *Inorg. Chem.*, 2009, **48**, 4207
9. L. Sun, S. Dang, J. Yu, J. Feng, L Shi and H. Zhang, *J. Phys. Chem. B*, 2010, **114**, 16393
10. Alessandro Sanguineti, Angelo Monguzzi, Gianfranco Vaccaro, Franco Meinardi, Elisabetta Ronchi, Massimo Moret, Ugo Cosentino, Giorgio Moro, Roberto Simonutti, Michele Mauri, Riccardo Tubino and Luca Beverina, *Phys. Chem. Chem. Phys.*, 2012, **14**, 6452
11. Evan R. Trivedi, Svetlana V. Eliseeva, Joseph Jankolovits, Marilyn M. Olmstead, Stéphane Petoud, and Vincent L. Pecoraro, *J. Am. Chem. Soc.* 2014, **1**, 1526
12. M. Rezaeivala, H. Keypour, *Coord. Chem. Rev.*, 2014, **280**, 203
13. W. Radecka-Paryzek, V. Patroniak, J. Lisowski, *Coord. Chem. Rev.*, 2004, **249**, 2156
14. L.-J. Xu, G.-T. Xu, Zh.-N. Chen, *Coord. Chem. Rev.*, 2014, **273–274**, 47
15. Z. Wang, W. Feng, P. Su, H. Liu, Zh. Zhang, Y. Zhang, T. Miao, X. Lü, D. Fang, W.-K. Wong, R. A. Jones, *Inorg. Chem. Comm.*, 2013, **36**, 11
16. T. Miao et al. / Spectrochimica Acta Part A: Molecular and Biomolecular Spectroscopy 132 (2014) 205–214

17. W.-X. Feng, Y.-N. Hui, G.-X. Shi, D. Zou, X.-Q. Lü, Ji-R. Song, D.-D. Fan, W.-K. Wong, R. A. Jones, *Inorg. Chem. Comm.*, 2012, **20**, 33
18. S. Chen, R.-Q. Fan, S. Gao, X. Wang, Y.-L. Yang, J. Lumin., 2014, **149**, 75
19. P. Gawryszewska, J. Lisowski, *Inorg. Chim. Acta*, 2012, **383**, 220
20. V.V. Utochnikova, O.V. Kotova, N.P. Kuzmina, *Mos. Univ. Bull. Chem.*, 2007, **48**, 277
21. A.S. Burlov, A.D. Garnovskii, V.A. Alekseenko, A.E. Mistryukov, V.S. Sergienko, V.G. Zaletov, V.V. Lukov, A.V. Khokhlov, M.A. Paray-Koshitz, *Russ. Coord. Chem.,* 1992, **18(8)**, 859
22. A.V. Meteliza, A.S. Burlov, S.O. Bezuglyi, A.D. Garnovskii, V.A. Bren, V.I. Minkin, N.N. Kharabaev, Patent RU2295527, 20.03.2007
23. A.V. Meteliza, A.S. Burlov, S.O. Bezuglyi, I.G. Borodkina, I.S. Vasilchenko, D.A. Garnovskii, S.A. Mashchenko, G.S. Borodkin, A.D. Garnovskii, V.I. Minkin, Patent RU2395512, 27.07.2010
24. Taylor R., Allen F. H. Statistical and Numerical Methods of Data Analysis / Structure Correlation : Weinheim : Verlag Chemie, 1994; Cambridge Structural Database, release 14
25. S. Shuvaev, V. V. Utochnikova, Ł. Marciniak, A. Freidzon, I. Sinev, R. V. Deun, R. O. Freire, Y. Zubavichus, W. Grünertd and N. P. Kuzmina, *Dalton Trans.,* 2014, **43**, 3121
26. G. Otting*, J Biomol NMR*, 2008, **42(1)**, 1
27. Sh. Hirata, Yu. Sakai, K. Masui, H. Tanaka, S. Y. Lee, H. Nomura, N. Nakamura, M. Yasumatsu, H. Nakanotani, Q. Zhang, K. Shizu, H. Miyazaki, Ch. Adachi, Nature Mater., 2015, **14**, 330
28. H. He, X. Zhu, A. Hou, J. Guo, W.-K. Wong, W.-Y. Wong, K.-F. Li and K.-W. Cheah, *Dalton Trans*., 2004, 4064
29. Martinus H.V. Werts, Ronald T.F. Jukes, Jan W. Verhoeven, *PCCP*, 2002, **4**, 1542
30. Yu.A. Zolotov, Osnovy analiticheskoj khimii (Basics of Analytical Chemistry), 2nd Ed., Vysshaja shkola, Moscow, 2000 (in Russian), p. 316.
31. N. N. Solodukhin, V. V. Utochnikova, L. S. Lepnev, N. P. Kuzmina, *Mend. Comm.*, 2014, **24(2)**, 91
32. Yu.A. Belousov, V.V. Utochnikova, S.S. Kuznetsov, M.N. Andreev, V.D. Dolzhenko, A.A. Drozdov, *Russ. J. Coord. Chem.,* 2014, **40(9)**, 627
33. H. Cariibano, Y. Guyot, C. Goutaudier, L. Laversenne and G. Boulon, *J. Phys. IV France*, 2004, **119**, 143
34. L.O. Meza Espinoza, "Pair driven IR fluorescence quenching of Yb in ZrO2:Yb", Master Thesis, 2006
35. A.Yu. Grishko, V.V. Utochnikova, A.A. Averin, A.V. Mironov, N.P. Kuzmina, *Eur. J. Inorg. Chem.,* 2015, **10**, 1660
36. G.M. Sheldrick, *Acta. Crystallogr*., 2008, **A64(1)**, 112